Optical properties and band bending of InGaAs/GaAsBi/InGaAs type-II quantum well grown by gas source molecular beam epitaxy

Wenwu Pan, Liyao Zhang, Liang Zhu, Yaoyao Li, Xiren Chen, Xiaoyan Wu, Fan Zhang, Jun Shao, and Shumin Wang

---

Articles you may be interested in

Study of molecular beam epitaxially grown InGaAsSbN/GaSb single quantum wells
J. Vac. Sci. Technol. B **29**, 03C112 (2011); 10.1116/1.3555368

On overannealing of GaIn(N)As/Ga(N)As multiple quantum wells grown by molecular beam epitaxy
J. Appl. Phys. **102**, 013504 (2007); 10.1063/1.2751483

Photoluminescence and photoreflectance study of InGaAs/AlAsSb quantum wells grown by molecular-beam epitaxy
J. Appl. Phys. **95**, 1050 (2004); 10.1063/1.1637936

Effect of temperature on the optical properties of GaAsSbN/GaAs single quantum wells grown by molecular-beam epitaxy
J. Appl. Phys. **93**, 4475 (2003); 10.1063/1.1560574

Long wavelength GaInNAs/GaAs quantum-well heterostructures grown by solid-source molecular-beam epitaxy
Appl. Phys. Lett. **77**, 2189 (2000); 10.1063/1.1314295

Optical properties and band bending of InGaAs/GaAsBi/InGaAs type-II quantum well grown by gas source molecular beam epitaxy

Wenwu Pan,[1,2] Liyao Zhang,[1,a)] Liang Zhu,[3] Yaoyao Li,[1] Xiren Chen,[3] Xiaoyan Wu,[1,2] Fan Zhang,[1,4] Jun Shao,[3] and Shumin Wang[1,5,b)]

[1]*State Key Laboratory of Functional Materials for Informatics, Shanghai Institute of Microsystem and Information Technology, CAS, 865 Changning Road, Shanghai 200050, China*
[2]*University of Chinese Academy of Sciences, Chinese Academy of Sciences, Beijing 100190, China*
[3]*National Laboratory for Infrared Physics, Chinese Academy of Sciences, 500 Yutian Road, Shanghai 200083, China*
[4]*School of Physical Science and Technology, ShanghaiTech University, Shanghai 201210, China*
[5]*Department of Microtechnology and Nanoscience, Chalmers University of Technology, Gothenburg 41296, Sweden*

Photoluminescence (PL) properties of $In_{0.2}Ga_{0.8}As/GaAs_{0.96}Bi_{0.04}/In_{0.2}Ga_{0.8}As$ quantum well (QW) grown on GaAs substrates by gas source molecular beam epitaxy were studied by varying excitation power and temperature, respectively. The type-II transition energy shifts from 1.149 eV to 1.192 eV when increasing the excitation power from 10 mW to 150 mW at 4.5 K, which was ascribed to the band-bending effect. On the other hand, the type-II PL quenches quickly along with fast redshift with the increasing temperature due to the relaxation of the band bending caused by the thermal excitation process. An 8 band $k \cdot p$ model was used to analyze the electronic properties and the band-bending effect in the type-II QW. The calculated subband levels and transition energy fit well with the experiment results, and two thermal activation energies of 8.7 meV and 50 meV, respectively, are deduced. *Published by AIP Publishing.* [http://dx.doi.org/10.1063/1.4962288]

I. INTRODUCTION

Recently, GaAsBi compounds have been considered to be promising materials for fiber-optic communication laser diodes with an efficient extension of light emitting wavelength, a relatively temperature-insensitive wavelength, and a reduction of Auger recombination.[1–3] The incorporation of a small amount of Bi atoms into GaAs strongly reduces the band-gap energy (84–91 meV/%Bi)[4–6] and, in addition, decreases the temperature coefficient of the band gap from 0.45 meV/K to about 0.15 meV/K.[2,7] For GaAsBi with Bi contents of above 10%, the spin–orbit splitting energy (Δ_{SO}) becomes larger than the band gap, and thus, the hot-hole-generating Auger recombination and the inter-valence band absorption processes are expected to be suppressed.[1,8,9] So far, light emitting diodes (LEDs) with $GaAs_{0.94}Bi_{0.06}$ as active regions have shown a good room-temperature electro-luminescence at about 1.20 μm.[10] Meanwhile, the electrically pumped GaAs-based lasers with three $GaAs_{0.94}Bi_{0.06}$ active quantum wells (QWs) have been fabricated successfully with the lasing wavelength up to 1.06 μm.[11] However, the room temperature emission at longer wavelengths by using conventional type-I GaAsBi QWs grown on GaAs is rather limited due primarily to the difficulty in incorporating a high content of Bi (>6%) and simultaneously retaining the high optical quality.[12–14] The reported maximum growth temperature for fabricating device in the molecular beam epitaxy (MBE) is about 380 °C, and only 4%–6% Bi is incorporated in the GaAsBi active layer.[2,11,15,16]

It is well known that the type-II band structure allows a QW with less lattice mismatch to achieve longer emission wavelength and the type-II heterostructures employing the InGaAs(N)/GaAsSb system on GaAs have been previously demonstrated to be promising for laser emitting at 1.55 μm.[17,18] Moreover, a type-II structure enables the energy band bending effect, which induces a blue shift in photoluminescence (PL) when the excitation power increases. Generally speaking, the mechanism of this effect has been discussed in terms of a triangular potential model in which the photo-generated electrons and holes form a dipole layer, creating a triangular-like potential at the interface,[19] while Jo *et al.*[20] found that the dominant contribution to the blueshift originates from the variation of the QW energy level after performing a self-consistent approach including the excitonic effect. On the other hand, the thermal escape of electrons from the GaAs well into the GaAsSb barrier is responsible for the PL quenching observed in the temperature dependent PL spectra of type-II GaAsSb/GaAs multiple quantum wells.[19]

Recently, we have grown the new type II InGaAs/GaAsBi/InGaAs QW by gas source MBE.[21] The emission wavelength was extended to 1070 nm at 4.5 K, longer than 943 nm and 1006 nm from the corresponding type-I InGaAs and GaAsBi QW, respectively. Our experimental and theoretical results show that this new kind of heterostructure may provide an interesting alternative to the type-I GaAsBi material for a near infrared generation. However, the spectroscopy property of this system has not been deeply explored. In this paper, the PL properties of the type II InGaAs/GaAsBi QW have been investigated by varying excitation power and temperature, respectively. Meanwhile, an 8 band

a)E-mail: lyzhang@mail.sim.ac.cn
b)E-mail: Shumin@mail.sim.ac.cn

k.p model combined with space charge effects was used to analyze the electronic properties and the bending effects observed in the experiment.

II. EXPERIMENTS

The type-II structure, which consists of 100 nm GaAs buffer/8.5 nm In$_{0.2}$Ga$_{0.8}$As/7.8 nm GaAs$_{0.96}$Bi$_{0.04}$/8.5 nm In$_{0.2}$Ga$_{0.8}$As/100 nm GaAs cap layers, was grown on semi-insulating GaAs (001) substrates using a V90 GSMBE system equipped with effusion cells for In, Ga, and Bi. As$_2$ was cracked from arsine at 1000 °C, its flux was controlled by regulating the gas pressure in the gas line, and the substrate temperature was measured by a thermocouple. For the growth of InGaAs/GaAsBi/InGaAs active region, the substrate temperature was decreased to 410 °C. No dislocations were observed during the high-resolution cross section TEM characterization, indicating such thick three-layer wells grown at low temperature remain elastically strain, and the details of the growth condition as well as the composition determination can be found elsewhere.[21] A diode pumped solid-state (DPSS) laser ($\lambda = 639$ nm) was used as the excitation source.

III. RESULTS AND DISCUSSION

A. Excitation-dependent PL

Figure 1 shows the 4.5 K PL spectra of the InGaAs/GaAsBi/InGaAs QW under different excitation intensities. Two peaks between 1.10 eV and 1.35 eV were observed. One peak located at 1.313 eV, labeled as P1, corresponds to the type-I transition in InGaAs layers, while the other peak at a lower energy with a much broader and intense feature, labeled as P2, originates from the type-II transition between the electrons in the InGaAs conduction band and holes confined in the GaAsBi valence band. When the incorporated Bi content reaches up to 4%, the valence band offset (VBO) of GaAsBi/InGaAs increases to such that most holes are confined in the GaAsBi layer causing the type-II radiative recombination. From the PL spectrum excited under a low power of 10 mW, it can be obtained that the energy difference between the peak P1(1.315 eV) and P2(1.149 eV) is about 166 meV, which is close to the estimated VBO of 169 meV for In$_{0.2}$Ga$_{0.8}$As/GaAs$_{0.96}$Bi$_{0.04}$ heterojunction.[21] The FWHM of the P2 are about 132 meV, which is much broader than the P1 of 25 meV. Such a broadening effect is related to the non-uniform distribution of Bi and/or Bi clusters in the GaAsBi layer.[22]
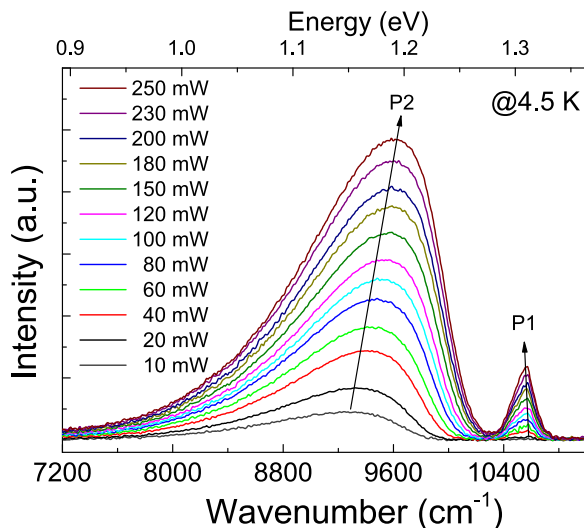
Surprisingly, we observed a giant blueshift under a moderate excitation intensity. As shown in Fig. 2, the PL peak energy of P2 has a shift of about 41 meV, and its FWHM increases when the pumping intensity changes from 10 to 200 mW, while those of P1 are almost not affected. The blueshift rate decreases, and its value as well as the FWHM eventually saturates to be about 1.192 eV and 143 meV, respectively, when the excitation power increases beyond 150 mW. This peculiar behavior cannot be ascribed to radiation heating, which should cause a shrinkage in the band gap. Also, the giant blueshift is hard to be assigned to the state filling of the localized states from the interface roughness or alloy potential fluctuations since it can be easily saturated at lower excitation power because of the low density of the localized states in comparison to the density of states for the QW ground states. In GaAsBi alloys, the carrier localization is a well-known phenomenon, and the so called S-shape behavior can be seen in the temperature dependent PL under the low excitation conditions.[23,24] In addition, Baranowski *et al.*[25,26] found that the PL kinetics are strongly influenced by the band bending effects as well as the carrier localization effects in type II GaAsSb/GaAs QWs using a time-resolved PL spectroscopy, suggesting that further investigations of the carrier localization phenomena in this InGaAs/GaAsBi QW are needed to evaluate its quality and perspectives for device applications. We believe that the underlying mechanism of the observations results from the band bending effect, which is intrinsic for the type-II band alignment of In$_{0.2}$Ga$_{0.8}$As/GaAs$_{0.96}$Bi$_{0.04}$ heterojunction, similar to the cases of GaAs/GaAsSb[19] and InGaAs/GaAsSb.[27] It is commonly accepted that the band-bending effect is caused by the spatial separation of the photo-excited or electrically pumped carriers in a

FIG. 1. The 4.5 K PL spectra of In$_{0.2}$Ga$_{0.8}$As/GaAs$_{0.96}$Bi$_{0.04}$/In$_{0.2}$Ga$_{0.8}$As QW under different excitation powers.
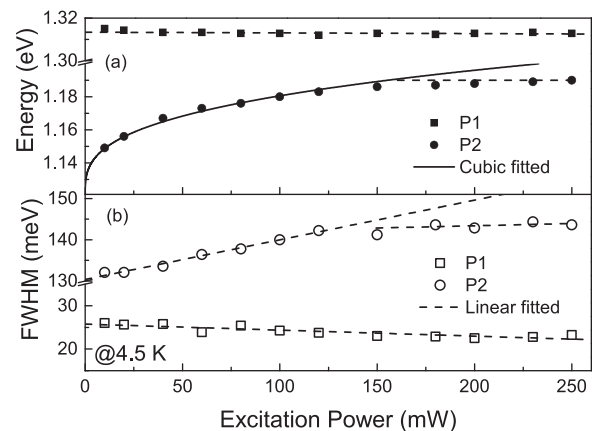
FIG. 2. The dependence of the peak energy (a) as well as the FWHM (b) of P1 and P2 on excitation power. A strong blueshift and saturation of P2 with the increase of excitation power are observed.
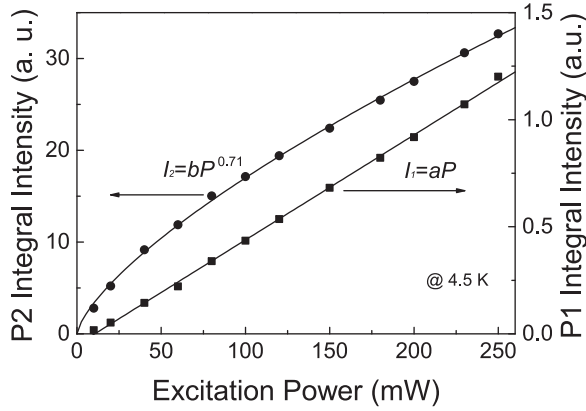
FIG. 3. The dependence of integral PL intensity of P1 and P2 on pumping power.

FIG. 4. The temperature dependent PL spectra of InGaAs/GaAsBi/InGaAs QW measured with a 120 mW excitation power.

type-II QW, in which the type-II transition energy is expected to increase proportionally with the third root of the excitation density due to the steepness raising of a triangular-like confining potential.[19] For the $In_{0.2}Ga_{0.8}As$/ GaAsBi type-II QW, electrons are confined in the InGaAs layer, and holes are localized in the GaAsBi layer. Indeed, a cubic curve as shown in Fig. 2(a) fits well with the experimental results with an excitation power below 150 mW. When the excitation power exceeds 150 mW, the energy blueshift as well as the FWHM broadening of P2 stops. This behavior can also be explained by the band bending model. Due to the band bending, there will be a potential barrier for electrons and holes in the GaAsBi and InGaAs layer, respectively. If the band bending is large enough, the barrier is able to prevent the photo-excited carriers from transferring from the high-energy band to the low-energy band, and the blueshift therefore saturates.

Figure 3 displays the dependence of integral PL intensities of P1 and P2, labeled as I_1 and I_2, on the pumping power P, respectively. We can see that the I_1 increases linearly while the I_2 shows a sublinear behavior with the increasing of P, respectively. For the semiconductor with a low background carrier density, the relationship between I and P can be reduced to a simple power law as $I \propto P^m$, where m = 1, 2, or 2/3 corresponds to radiative, Shockley-Read-Hall nonradiative, and Auger recombination, respectively.[28] The slope of the plot in Fig. 3 is fitted as m = 1 and 0.71 for P1 and P2, respectively, which indicates that the dominant carrier recombination mechanisms for the InGaAs/GaABi type II QW mainly include radiative and Auger recombination at 4.5 K.

B. Temperature-dependent PL

Figure 4 shows the temperature dependent PL spectra with a fixed excitation of 120 mW measured at temperature varying from 4.5 K to 290 K. We can see that both the peak energy and intensity of P1 and P2 decrease with the increasing temperature. Especially for P2, the PL intensity decreases gradually with the increasing temperature from 4.5 K to 130 K and then quenches quickly when temperature increases beyond 160 K. In addition, compared with the 41 meV redshift of P1, a larger redshift of P2, i.e., 84 meV as
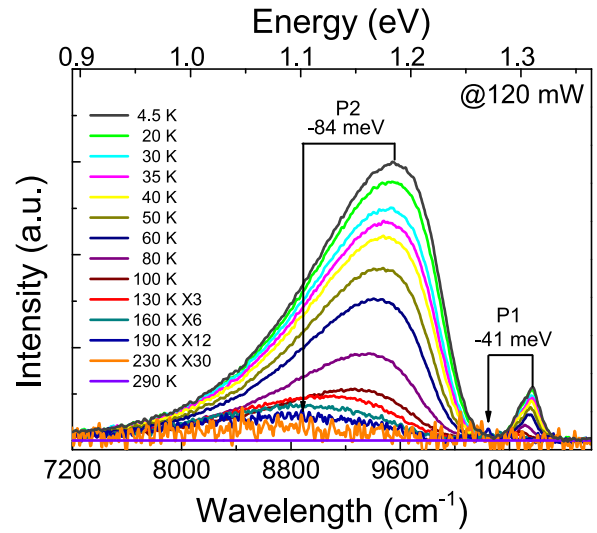
illustrated in Fig. 4, was found when increasing the temperature from 4.5 K to 190 K. The energies and FWHMs of P1 and P2 are summarized in Fig. 5, and no obvious S-shape behaviors of the two peaks are observed at a low temperature, indicating the carrier localization effect maybe saturated at this excitation conditions. For the peak energy of P1, it can be analyzed using the Varshni relationship[29] of

$$E = E_0 - \alpha T^2/(\beta + T), \quad (1)$$

where E_0 is the fundamental excitonic transition energy at absolute zero temperature, α and β are the adjustable parameters. The constant α is related to the electron-phonon interaction, and β is closely related to the Debye temperature. As shown in Fig. 5(a), for P1, the best fit to the experimental data is obtained with $\alpha = 0.486$ meV/K, $\beta = 197$ K, and $E_0 = 1.313$ eV. The values of α and β are very close to those of bulk $In_{0.2}Ga_{0.8}As$.[30] However, for P2, with temperature increasing from 60 K to 160 K, a much faster redshift was observed. The FWHM of P2 remains at around 140 meV for $T < 60$ K and almost increases linearly with temperature for 60 K $< T < 160$ K, while that of P1 is almost not affected in
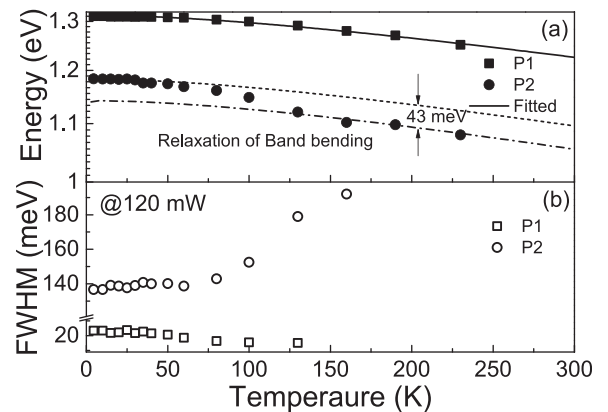
FIG. 5. Dependence of the PL peak energy as well as FWHM of P1 and P2 on temperature.

the temperature range up to 130 K as shown in Fig. 5(b). The redshift cannot be explained by the thermal population of the electron and hole states with high-k values, which have a high probability of radiative recombination since the PL maxima should shift to higher-photon energies relative to the effective band-gap energy. This behavior is also related to the band bending effects in type-II QWs, where the quantum confinement becomes less pronounced with the increasing temperature. At a high temperature, the ability of the triangular-like potential to confine carriers is reduced since the photo-excited carriers can be thermally excited to escape from the InGaAs/GaAsBi interface. The relaxation of the band bending leads to a much faster reduction of effective band gap in the type-II QW than that of in bulk or a normal type-I QW like InGaAs. As shown in Fig. 5, about a 43 meV redshift contribution by band bending relaxation is deduced by comparing the temperature dependent behaviors between P1 and P2. Thus, the flat-band transition energy of P2 is estimated to be 1.142 meV at 4.5 K. In Fig. 6, we display the Arrhenius plots of the intensity as well as the integral intensity of the P1 and P2, respectively. The solid lines are calculated by the expression

$$I = I_0/(1 + C_1 e^{-E_1/kT} + C_2 e^{-E_2/kT}),\qquad(2)$$

where I_0 is the integral PL intensity at 0 K, C_1 and C_2 are constants, and E_1 and E_2 are the thermal activation energies. For the integral intensity of P2, as depicted in Fig. 6, the obtained E_1 and E_2 values of the PL quenching are 8.7 meV and 50.0 meV, respectively. It should be noted that the deduced thermal activation energy of E_1 is sensitive to the accuracy of PL data obtained in the low temperature range, while E_2 is sensitive to the certainty of the PL data measured at a relatively high temperature. Thus, a similar value of E_1, i.e., 8.4 meV, is deduced from the temperature dependence of the integral intensity of P1 as the line shapes of P1 measured at T < 100 K are fixed as shown in Fig. 4. However, the weak PL features of P1 measured beyond 100 K lead to a large deviation when deducing the thermal activation energy of E_2. The origination of the two thermal activation energies of E_1 and E_2 will be discussed later.
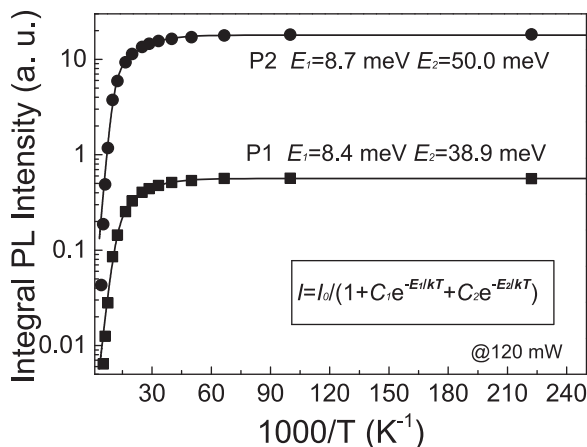
C. Electronic properties

In order to interpret the band bending effect and the PL quench observed in our experimental results, it is necessary to calculate the energy levels and wave-functions under different injection levels for the structure described above. Thus, a semi-quantitative analysis of the band bending based on the 8 band $\boldsymbol{k.p}$ model has been performed. In the calculations reported in this paper, band offset ratios of 60:40 between the strained InGaAs and GaAs and 24:76 between the strained GaAsBi and GaAs were used, respectively.[6,31] The transformation of GaAsBi and $In_{0.2}Ga_{0.8}As$ to form a type-II configuration from a type-I configuration is estimated to occur near a Bi concentration of 1.3%. A schematic diagram of the conduction and valence bands in the active region of our structure is shown in Fig. 7(a), where the valence band edge of GaAs is taken to be zero energy. The GaAsBi hole QW, which is 7.8 nm thick and has a nominal Bi content of 4%, is sandwiched between the two 8.5 nm $In_{0.2}Ga_{0.8}As$ electron QWs. We have used the material parameters[21] to solve Schrödinger's equation for flat band conditions as well as for carrier injection by performing self-consistent calculations. The calculated energy levels within the schematic band diagram and the selected envelope wave functions are shown in Fig. 7.

For the flat band, as shown in Fig. 7(a), in the conduction band, the thin GaAsBi layer allows the electron wave-functions in the InGaAs QWs to couple, resulting in two coupled solutions, symmetric (e1S = 1.403 eV) and anti-symmetric (e1A = 1.408 eV), which are confined in the InGaAs QWs. The first electron excited sate (e2 = 1.465 eV) shows localized features in GaAsBi layer. In the valence band, the heavy and light hole solutions are strongly confined to the GaAsBi layer. The calculations show that, due to the difference in the heavy and light hole masses, two heavy hole energy levels (HH1 = 0.239 eV; HH2 = 0.203 eV) occur in the GaAsBi QW at lower energy than the first light hole solution (LH1 = 0.178 eV). In the InGaAs layer, the first heavy hole solution (hh1 = 0.072 eV) is confined in the

FIG. 6. Logarithm of the PL and PL integral intensity of P1 and P2 versus reciprocal temperature together with the respective activation energy fit.
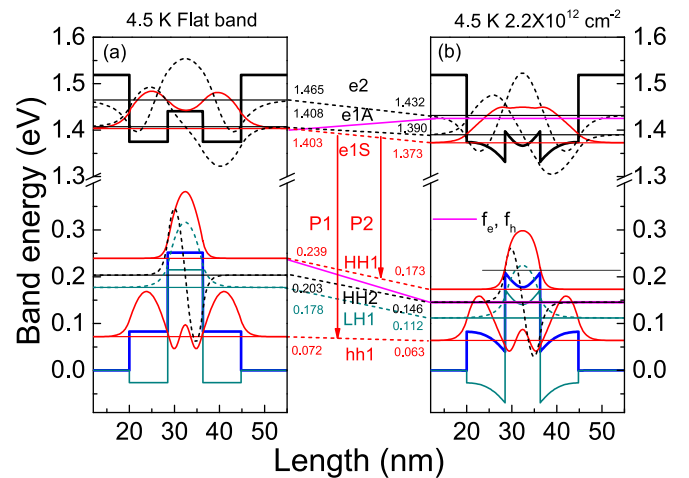
FIG. 7. The 4.5 K bulk bandedge profiles and selected wave functions calculated for flat band (a) and injecting e-h density 2.2 × 10^{-2} cm^{-2} (b). Legends for wave functions and the corresponding electron and hole sub-band energy levels are depicted in the figure.

InGaAs QWs. The type-I transition energy between e1S and hh1 with an overlap of 93% is 1.331 eV. The 29% overlap of the wave-functions enables the type-II transitions between the e1S and the HH1 with a transition energy of 1.164 eV. Both the transition energy values are about 20 meV larger than the experimental observation discussed previously, i.e., 1.313 eV and 1.142 eV, respectively. The deviation may result from the underestimation of about 2% In content in the InGaAs layers.

For the band bending, we consider the change of the non-equilibrium carrier density due to photo-excitation. As shown in Fig. 7(b), when the injected e-h pair density increases to 2.2×10^{12} cm^{-2}, two approximately triangular wells are produced due to the strong band bending near the InGaAs/GaAsBi interface. Meanwhile, the quasi-Fermi level of the photo-generated electrons (f_e) has not exceed the e2, while that of holes (f_h) is just reaching to the 2HH subband level, indicating that the photo-excited electrons and holes are majorly accumulated in the InGaAs and GaAsBi, respectively, and the band bending will be triggered when there is a further increase in the e-h density. Due to the band bending effect, both the electron and the hole subband levels decrease. However, the HH1 subband level shift is larger than the e1S subband level, and as a result, the transition energy of P2 shows a blueshift about 36 meV. Meanwhile, it should be noted that, with the increasing of the band-bending effects, the wave functions of the e1S and 1HH states will penetrate further into each other, and thus, the ground electron and hole wavefunctions become less spatially separated and the structure tends to be type-I. This is the reason that the blueshift rate of P2 will be slowed down and the peak energy of P2 will be saturated at a high excitation power.

It should be noted that the band bending model based on the $k \cdot p$ method works in the case of low temperature since the thermal activation process of the injected carriers is not considered. The temperature dependent PL behavior summarized in Fig. 4 shows that the band bending can be relaxed when the temperature increases up to 160 K due to the thermal activation of carriers. In addition, two activation energies of $E_1 = 8.7$ meV and $E_2 = 50.0$ meV, which are deduced from the temperature dependent integral intensity of P2, are close to the value of the energy difference between e1S and the e1A (5 meV), and the first delocalized state e2 (62 meV) as indicated in Fig. 7. This implies that the thermal escape of electrons from the ground state localized near the InGaAs/GaAsBi interface into the whole QW is responsible for the PL quenching in the InGaAs/GaAsBi/InGaAs QW near room temperature. Thus, we can expect that increasing In content should be useful for the room temperature PL emission of the InGaAs/GaAsBi type II QW due to the improvement of electron confinement. Furthermore, for the fact that no PL at room temperature was observed in the type II InGaAs/GaAsBi QW under the excitation of 120 mW, a great number of non-radiative centers, produced during the low temperature growth of the active region, are also probably responsible for this issue. Further optimization of the growth conditions, such as increasing the growth temperature of the two InGaAs layers, is needed to reduce the non-

radiative centers and improve the material quality for device applications.

Figure 8(a) shows the subband energies as well as quasi-Fermi levels as a function of the injected e-h sheet density based on the calculation. Also, the calculated energy shifts of P1 and P2 are also shown in Fig. 8(b). The blueshift of P2 is about 36 meV and 40 meV when the f_h and the f_e just exceed the HH2 and e1A subbands, respectively. With a further increase of injecting density to 4×10^{12} cm^{-2} as shown in Fig. 8, the blueshift of the transition energy P2 due to the strong band bending tends to be saturate at 48 meV, which is close to the experiment observation of 50 meV. For the type I transition P1, the calculation results suggest a redshift due to the band bending effect, which is not consistent with the excitation power dependent PL spectra as shown in Fig. 1. As reported in Ref. 21, the Bi segregation in the growth direction takes place, and the maximum Bi concentration appears at much closer to the upper InGaAs/GaAsBi interface. This is caused by the relatively high growth temperature for GaAsBi since the Bi surface segregation can be enhanced with the increasing growth temperature.[32] The transition of P1 we observed most likely originates from the lower InGaAs layer where the possibility of achieving the type II band alignment in the lower GaAsBi/InGaAs interface is small, and thus, the band bending effect is negligible. If the P1 originates from the upper type II InGaAs/GaAsBi quantum well, the relaxation of the band bending will slow down the redshift of P1, while this was not observed in the temperature dependent PL, and further work is required to confirm it.

IV. SUMMARY

In summary, we have reported several peculiar behaviors in the PL spectra of InGaAs/GaAsBi type II QWs related to the band bending caused by the dipole formation by
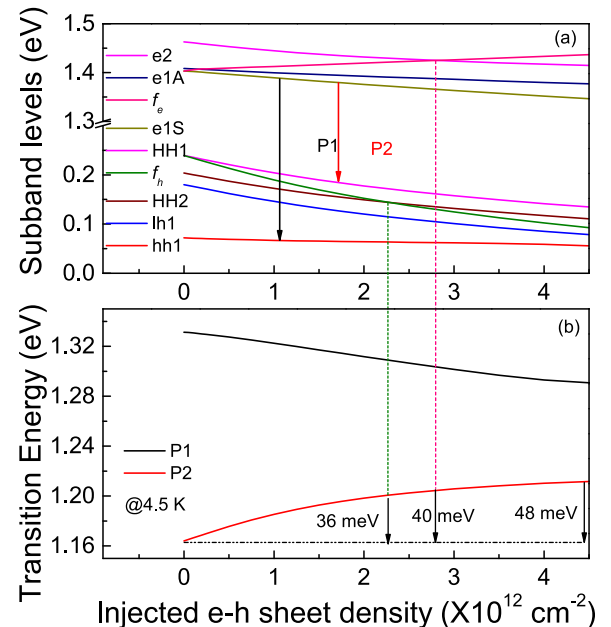
FIG. 8. The calculated changes of subband energy levels and the quasi-Fermi levels with varying e-h sheet density injected in the InGaAs/GaAsBi/InGaAs QW based on the 8 $k \cdot p$ model (a). The calculated transition energies of P1 and P2 are also plotted (b).

separation of electrons and holes, including a giant blueshift, a saturation effect, and the relaxation of band bending due to the thermal excitation process. The experimental results are well explained by the $k \cdot p$ model. Our results are instructive for understanding the optical properties in the InGaAs/GaAsBi type-II semiconductor heterostructures.

ACKNOWLEDGMENTS

[1] C. A. Broderick, M. Usman, S. J. Sweeney, and E. P. O'Reilly, Semicond. Sci. Technol. **27**, 094011 (2012).
[2] T. Fuyuki, K. Yoshida, R. Yoshioka, and M. Yoshimoto, Appl. Phys. Express **7**, 082101 (2014).
[3] S. J. Sweeney and S. R. Jin, J. Appl. Phys. **113**, 043110 (2013).
[4] S. Tixier, M. Adamcyk, T. Tiedje, S. Francoeur, A. Mascarenhas, P. Wei, and F. Schiettekatte, Appl. Phys. Lett. **82**, 2245 (2003).
[5] S. Francoeur, M. J. Seong, A. Mascarenhas, S. Tixier, M. Adamcyk, and T. Tiedje, Appl. Phys. Lett. **82**, 3874 (2003).
[6] M. P. Polak, P. Scharoch, and R. Kudrawiec, Semicond. Sci. Technol. **30**, 094001 (2015).
[7] J. Yoshida, T. Kita, O. Wada, and K. Oe, Jpn. J. Appl. Phys., Part 1 **42**, 371 (2003).
[8] B. Fluegel, S. Francoeur, A. Mascarenhas, S. Tixier, E. C. Young, and T. Tiedje, Phys. Rev. Lett. **97**, 067205 (2006).
[9] K. Alberi, O. D. Dubon, W. Walukiewicz, K. M. Yu, K. Bertulis, and A. Krotkus, Appl. Phys. Lett. **91**, 051909 (2007).
[10] R. D. Richards, A. R. Mohmad, J. P. R. David, C. J. Hunter, and F. Bastiman, IET Optoelectron. **10**, 34 (2016).
[11] R. Butkute, A. Geizutis, V. Pacebutas, B. Cechavicius, V. Bukauskas, R. Kundrotas, P. Ludewig, K. Volz, and A. Krotkus, Electron. Lett. **50**, 1155 (2014).
[12] M. Yoshimoto, S. Murata, A. Chayahara, Y. Horino, J. Saraie, and K. Oe, Jpn. J. Appl. Phys., Part 2 **42**, L1235 (2003).
[13] V. Bahrami-Yekta, T. Tiedje, and M. Masnadi-Shirazi, Semicond. Sci. Technol. **30**, 094007 (2015).
[14] W. Bennarndt, G. Boehm, and M. C. Amann, J. Cryst. Growth **436**, 56 (2016).
[15] C. J. Hunter, F. Bastiman, A. R. Mohmad, R. Richards, J. S. Ng, S. J. Sweeney, and J. P. R. David, IEEE Photonics Technol. Lett. **24**, 2191 (2012).
[16] T. Fuyuki, R. Yoshioka, K. Yoshida, and M. Yoshimoto, Appl. Phys. Lett. **103**, 202105 (2013).
[17] I. Vurgaftman, J. R. Meyer, N. Tansu, and L. J. Mawst, Appl. Phys. Lett. **83**, 2742 (2003).
[18] B. Chen, A. L. Holmes, V. Khalfin, I. Kudryashov, and B. M. Onat, Laser Technology for Defense and Security VIII **8381**, 83810F (2012).
[19] Y. S. Chiu, M. H. Ya, W. S. Su, and Y. F. Chen, J. Appl. Phys. **92**, 5810 (2002).
[20] M. Jo, M. Sato, S. Miyamura, H. Sasakura, H. Kumano, and I. Suemune, Nanoscale Res. Lett. **7**, 1 (2012).
[21] See https://arxiv.org/abs/1606.04657 for information about the structural properties of the sample.
[22] A. R. Mohmad, F. Bastiman, C. J. Hunter, J. S. Ng, S. J. Sweeney, and J. P. R. David, Appl. Phys. Lett. **99**, 042107 (2011).
[23] R. Kudrawiec, M. Syperek, P. Poloczek, J. Misiewicz, R. H. Mari, M. Shafi, M. Henini, Y. G. Gobato, S. V. Novikov, J. Ibanez, M. Schmidbauer, and S. I. Molina, J. Appl. Phys. **106**, 023518 (2009).
[24] S. Imhof, A. Thranhardt, A. Chernikov, M. Koch, N. S. Koster, K. Kolata, S. Chatterjee, S. W. Koch, X. F. Lu, S. R. Johnson, D. A. Beaton, T. Tiedje, and O. Rubel, Appl. Phys. Lett. **96**, 131115 (2010).
[25] M. Baranowski, M. Syperek, R. Kudrawiec, J. Misiewicz, J. A. Gupta, X. Wu, and R. Wang, Appl. Phys. Lett. **98**, 061910 (2011).
[26] M. Baranowski, M. Syperek, R. Kudrawiec, J. Misiewicz, J. A. Gupta, X. Wu, and R. Wang, J. Phys.: Condens. Matter **24**, 185801 (2012).
[27] J. Hu, X. G. Xu, J. A. H. Stotz, S. P. Watkins, A. E. Curzon, M. L. W. Thewalt, N. Matine, and C. R. Bolognesi, Appl. Phys. Lett. **73**, 2799 (1998).
[28] I. P. Seetoh, C. B. Soh, E. A. Fitzgerald, and S. J. Chua, Appl. Phys. Lett. **102**, 101112 (2013).
[29] Y. P. Varshni, Physica **34**, 149 (1967).
[30] I. Vurgaftman, J. R. Meyer, and L. R. Ram-Mohan, J. Appl. Phys. **89**, 5815 (2001).
[31] J. P. Reithmaier, R. Hoüger, H. Riechert, A. Heberle, G. Abstreiter, and G. Weimann, Appl. Phys. Lett. **56**, 536 (1990).
[32] E. Luna, M. Wu, M. Hanke, J. Puustinen, M. Guina, and A. Trampert, Nanotechnology **27**, 325603 (2016).